Sujatha and Selvathi *EURASIP Journal on Image and Video Processing* (2015) 2015:8
DOI 10.1186/s13640-015-0062-9

EURASIP Journal on Image and Video Processing
a SpringerOpen Journal

RESEARCH Open Access

Connected component-based technique for automatic extraction of road centerline in high resolution satellite images

Chinnathevar Sujatha[1*] and Dharmar Selvathi[2]

Abstract

In remote sensing analysis, automatic extraction of road network from satellite or aerial images can be a most needed approach for efficient road database creation, refinement, and updating. In this paper, a method for automatic extraction of road centerline from high resolution satellite image is proposed. The proposed work consists of three stages: segmentation of road region, connected component-based operations used to extract the connected road component from segmented road region, and removal of unwanted non-road pixels using morphological operation. The proposed algorithm is implemented on various satellite images, and the results are given in this work. The performance of the proposed method is evaluated by comparing the results with ground truth road map as reference data, and performance measures such as completeness, correctness, and quality are calculated. The average value of completeness, correctness, and quality of various images are 90%, 96%, and 87%, respectively. These measures prove that the proposed work yields road network very closer to reference road map. The proposed method yields very good result for noisy image also, and it proved that the proposed method is insensitive for noise. Performance measures of the proposed work are compared with other methods, and this comparison proves that the proposed method yields very good results than other methods.

Keywords: Road extraction; High resolution satellite image; Connected component; Morphological operation; Trivial opening; Completeness; Correctness; Quality

1 Introduction

Automatic detection of road networks from the satellite and aerial images is the most demanded research subject, and it is used for many remote sensing applications. Geographic information system (GIS) needs an automatic road extraction process for updating their data [1]. Manual updating of GIS database is costly, time-consuming process, and also there is a possibility of error in manual updating of road network [2-4]. Therefore, automatic road feature extraction from high resolution satellite image is required to detect the road network in a robust manner. Road data enables GIS applications to facilitate a variety of services which include satellite navigation, route planning, health-care accessibility planning, land cover classification, and infrastructure management. The objective of road feature extraction method is providing a binary mask in which true pixels represent road regions, and false pixels indicate non-road regions. The major problem of road extraction method is the complex structure of the images, which contain many different objects, such as roads, houses, trees, vehicles, etc., with differences in shape, tone, and the texture.

Road extraction methods can be classified into two categories such as semi-automatic and fully automatic [5]. The road detection methods which are requiring human interaction are classified as semi-automatic, and those that are not requiring human interaction are known as automatic [6]. Though many researchers are developing their own algorithm for road detection, some of the works are semi-automatic [7-11] which is not suitable for real-time application and other works are automatic road detection system [12-27]. All the work has its own merits and demerits. Some of the existing

* Correspondence: sssujathac@yahoo.co.in
[1]Department of Electronics and Communication Engineering, Sethu Institute of Technology, Madurai-Thoothukudi Highway, Kariapatti, Virudhunagar District 626115, Tamil Nadu, India
Full list of author information is available at the end of the article

automatic road extraction works based on various approaches are discussed in this chapter.

Jiuxiang et al. presented a method for automatic road extraction which includes three steps: road seed pixel is identified and then road tracking and growing of road segment. This method used a concept of road footprints to compute the probability that a pixel is located on a road. A road tree is then constructed to identify the road network [1]. Cem et al. proposed a road extraction system based on probabilistic and graph theory [2]. Edge pixel is extracted. Then, using probabilistic method, road centerline is extracted. Finally, graph theory is used to represent the extracted road segments in a graph formation. This system depends on the edge information of an image [2]. Xiaoying et al. integrated two detectors to detect road centerlines. The outputs of fine-scale image segmentation-based detector and fuzzy-based multiscale curvilinear detector are combined together to get road network, and path searching algorithm is used for this integration [3]. Another road extraction system proposed by Zhijian et al. is also based on two methods [4]. This system is implemented by cross-validating line features of the line segment detector (LSD) and the statistical region merge (SRM) according to their spatial relationship.

Xiangguo et al. classified the road into with salient road marking and without salient road marking, then multiple road tracking systems are used to detect road network. The least squares interlaced template matching is used to extract ribbon road networks with salient road markings, profile matching, rectangular template matching, and parallelepiped angular texture signature and are combined to extract ribbon roads without salient lane markings [5]. Dal et al. proposed an automatic road extraction method which included two steps: first step is road seed extraction-based geometric and radiometric properties of an image, and the next step is linking of road seeds based on two basic perceptual grouping rules, the proximity and collinearity rules [6]. A method for road centerline extraction based on shape features and multivariate adaptive regression splines is presented by Zelang et al. [12]. This method consists of four stages: segmentation of remotely sensed image; then extraction of road region based on shape and spectral feature; after that, application of multivariate adaptive regression splines to extract road centerline; finally, the use of connection algorithm to get complete road network. Performance measures are calculated, and results are tabulated. Automatic road detection in urban region based on structural, spectral, and geometric characteristics of road is proposed by Senthilnath et al. [13]. The main steps of this work are preprocessing to reduce the unwanted objects and extraction of road segments using texture progressive analysis and normalized cut method. The performance evaluation is measured by comparing the results with reference road map, and the values are given.

A support vector machine-based road centerline is proposed by Xin et al. [14]. This algorithm used both geometrical features of road and spectral variation, and hybrid of geometrical and spectral information is analyzed using SVM classifier. This algorithm is implemented on two IKONOS multispectral datasets. A hybrid method for road network detection in both rural and urban areas is presented by Hang et al. [15]. Thresholding based on homogeneity histogram along with Gabor filter is used for road surface and lane marking segmentation in rural images. Road surface in urban area is extracted with SVM classifier, and Gabor filter is used for further refinement. Experimental results are obtained from some satellite images. Automatic road extraction from multispectral satellite images based on predominant features of road is presented by Sukhendu et al. [16]. Probabilistic Support Vector Machines and Dominant Singular Measures are used to segment the road regions, and multistage post- processing is done to remove non-road parts. Finally, the author solved the discontinuity problems.

A road centerline detection using wavelet transform from high resolution remote sensing images is presented by Tieling et al. [17]. This work consists of two parts. Initially, road edges are extracted using two-dimensional wavelet transform. After that, thinning algorithm is applied to detect thin centerline of road network.

Sahar et al. proposed a road extraction algorithm on satellite images using particle filter and extended Kalman filter [18]. Extended Kalman filter along with particle filter is applied to trace the road beyond obstacles and to follow different road branches after road junction is found. The proposed result is compared with manually drawn roads. An integrated approach for road network segmentation in satellite images is proposed by Thierry et al. [19]. This method includes three stages. Initially, image is filtered using watershed transform to remove non-road areas. Then, area closing operator is applied to extract the road network structure. After that, a graph describing the adjacency relationship between watershed lines is built. Finally, Markov random field is defined upon this graph to extract road network in satellite images. Mena et al. proposed an approach for automatic road extraction in rural and semi-urban areas which includes four modules: data preprocessing, binary segmentation based on texture progressive analysis, vectorization of the binary image by means of skeletal extraction and morphological operations, and finally evaluation of the proposed system by comparing with manually drawn road map [20].

Zelang et al. [21] proposed a method for road centerline extraction from classified image which consists of the three stages: feature points are extracted using tensor voting, kernel density estimation is used to find probability of each pixel being located on the road centerline, and feature points are projected onto ridge lines using the subspace constrained mean shift method. Centerline of the road is formed by linking the projected feature using geodesic method. The performance of this method is proved by comparing the quantitative measures with other methods [21]. Wenzhong et al. presented road extraction method for urban area which includes two stages; image is classified as road class and non-road class using path openings and closings, and road images are refined by shape features. The performance measures are evaluated, and this is compared with other methods [22]. A directional morphological operator based on road segmentation approach is proposed by Valero et al. [23]. For each pixel, they construct a morphological profile using path opening and path closing morphological operations which is used for road extraction and author used pixel-based approach for road extraction. Experimental results for some satellite images are given. Pankaj et al. proposed a road network segmentation technique using adaptive global thresholding along with morphological operations [24]. Road regions are segmented using average intensity values, and morphological operators are used for further processing. They gave experimental result for an image and evaluated their work by measuring quality parameters.

Rohit et al. proposed a method for road extraction using morphological and K-means clustering [25]. Road regions are separated from high resolution image using K-means clustering. This segmented region consists of some non-road pixels, and those pixels are removed using a morphological operator. The results are proved by evaluating the quality measures. Road network recognition approach using image morphological characteristics is proposed by Zhu et al. [26]. This work is based on morphological operations and a line segment match method. By using grayscale, morphological characteristic outline of road network is detected and basic road network is detected using line segment match method. The road network is further processed based on binary morphology and road knowledge. The accuracy of proposed approach is proved by calculating the quantitative measures. Automatic road extraction method using road intersection model is presented by Boshir et al. [27]. The entire process of road intersection detection is divided into two sequential modules. First module is detection of road network using different morphological direction filter, and second module is extraction of road intersection to determine road orientation. Algorithm is implemented on various images, and correctness values are measured for evaluating this method [27].

An image contains more number of connected components (CC), and each connected component is a set of pixels in which each pair of pixels is connected [28]. Trivial opening is used to filter the sets of CC of an image based on certain condition [29]. The connected component is preserved, if the condition is satisfied; otherwise, that component is removed [28,29]. Trivial opening is used for road extraction [30-32]. A hybrid method of using artificial neural network, contour tracing algorithm, and morphological trivial opening is used to extract road from remotely sensed image and is presented by Sowmya et al. [30]. This algorithm is evaluated by measuring the quality measures. An approach based on fuzzy logic and trivial opening is proposed; to extract main road centerlines from pan-sharpened IKONOS images, it is presented by Ali et al. [31]. An approach to detect road network from high resolution image using combination of a developed fuzzy system and trivial opening is proposed by Mohammadzadeh et al. [32].

After reviewing the existing work on road extraction, some works are semi-automatic [7-11] which is not suitable for real-time application. Some other works need fuzzy optimization technique [3,31,32], and some other works are based on wavelet transform [17,19] and support vector machine [14-16]. In those cases, complexity of algorithm is high. In some of algorithm based on seed-based approach [1,6,18], this work reliability is based on the road seed pixels. In few cases, combination of two or more algorithm was used for road extraction [4,5,22]. Some of the works are used for segmenting road region and not used for centerline extraction [13,23-25].

Morphological operators play a vital role in road segmentation from satellite image. The computational cost of morphological-based road extraction is lesser than wavelet-based approach and support vector machine-based approach; thus, morphological operator and trivial operator are mainly used for road extraction. The proposed work of this paper is road centerline extraction using connected component-based extraction along with morphological operator. Thus, the proposed method is a hybrid method of connected component analysis and morphological operator. This proposed hybrid method yields very good results than simple morphological approach. Optimization technique is not needed for this proposed work, result is not based on seed, and complexity is lesser than wavelet-based approaches.

Most of the existing morphological-based methods extract the road region only, and some other methods of road linking is needed to get continuous roads; but in this proposed work, road centerline is extracted and road linking is not needed. Fine single pixel width road centerline is extracted using proposed methods. Existing methods are not implemented on noisy image;

but proposed work is implemented on noise image, and very good result is obtained. Performance measures are evaluated to prove the quality of the proposed work. Thus, noise-immune automatic extraction of road centerline using connected component-based morphological operation is proposed in this paper. The remaining part of this paper consists of Section 2 which discusses about the methodology of proposed road extraction method. Section 3 provides the experimental results and discussion. Section 4 gives conclusion of the work.

2 Methodology of proposed work

This proposed work for automatic road centerline extraction method from high resolution satellite image is based on connected component extraction and morphological operators. The detailed methodology of proposed work is given in Figure 1. This methodology includes adaptive global thresholding method, connected component analysis, morphological closing, dilation, morphological thinning, and further refinement for removal of small edge segments and performance measures.

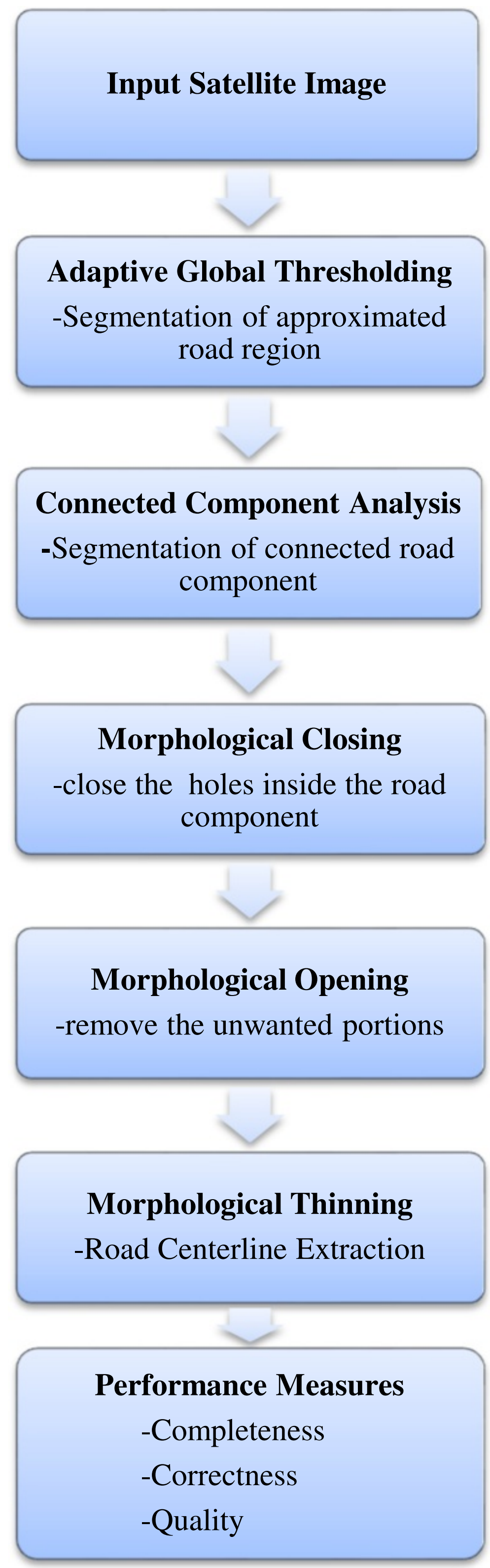

Figure 1 Methodology of proposed work.

2.1 Adaptive global thresholding

Satellite image is converted into gray image, and road region is segmented from that image using histogram analysis. Adaptive global thresholding is applied to remove the non-road pixels and segment-approximated road region from the satellite image [24]. The histogram of the satellite image is analyzed and divided into four main sections to obtain the desired threshold value for segmentation. The test image 1 and its histogram are given in Figure 2a and b, respectively.

The histograms are divided based on mean value (M) of all the pixel intensity values in an image. Section A includes the pixels having the intensity values lies between lowest intensity values to half of mean value (M). This section identifies dark objects of an image such as dark vehicles, shadows, lake, muddy ponds, etc. Section B groups the pixels having intensities from half of the M value to M value, and this section identifies dark gray shade objects like trees, grasslands, etc. Section C includes the pixels from M value to half of maximum intensities, and these pixels belong to bright gray objects such as roads, lane markers, etc. Section D groups the pixels that lie between half of maximum intensity and maximum intensity, and this section can identify bright objects like concrete cement road, bright vehicles, etc. This approach is used in the case where single value thresholding will not function properly, since the threshold value of pixel depends on its position within an image. Therefore, this technique is called as adaptive global thresholding. From this technique, approximated road regions are identified. The pixels that lie in that region are assigned to value 1 and all the remaining pixels

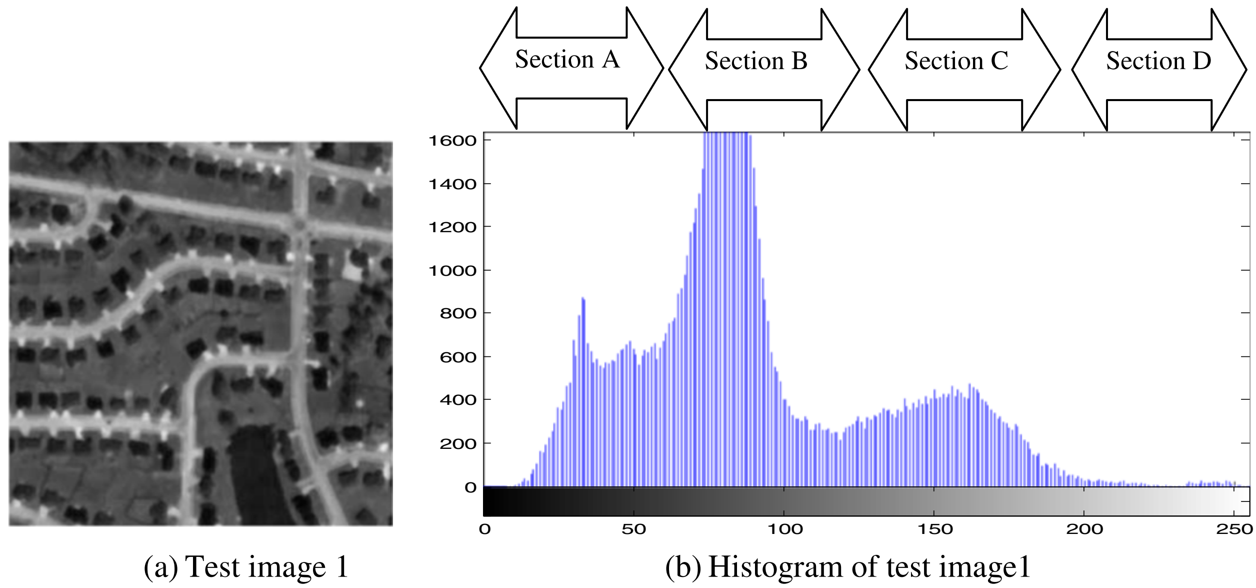

Figure 2 Test image 1 (a) and histogram of test image 1 (b).

are made to 0. Now, gray image is converted into binary image in which road regions appeared in white and all other pixels appeared in black.

2.2 Connected component analysis

For any pixel in an image, the set of pixels that is connected to that pixel is called connected component of an image [28]. Any set of pixels which is not separated by a boundary is called connected pixels. Each maximal region of connected pixels is called a connected component. The connected components partition an image into segments. The analysis of connected components is mainly used for many automated image processing applications such as object extraction, road map extraction, line detection, etc. Connected components can be extracted using morphological operations. Connected components of an image can be extracted by combining dilation and the mathematical intersection operation. Let Y be an image, and connected component in an image is denoted as A; and a known point of A is denoted as p which is assigned to $X0$. Then, the following expression (Equation 1) gives all the elements of A.

$$X_k = (X_{k-1} \oplus B) \cap Y \quad k = 1, 2, 3, \ldots \tag{1}$$

Where the symbol $\oplus$ represents morphological dilation, $\cap$ represents intersection, and B is a suitable structuring element. If $X_k = X_{k-1}$, then the algorithm has converged and let $A = X_k$.

Trivial opening is defined by Jean et al. [33], and it is used to extract the connected components based on some criteria. Let Y be an image, $\{Y(n) \mid n = 1, 2, 3, \ldots, N\}$ is a sequence of connected components in the image Y, and $y(i)$ is a point in $Y(i)$. The trivial opening can be defined with a condition T, as follows in Equation 2.

$$\tau_O(y) = \begin{cases} Y(i), \textit{ if } Y(i) \textit{satisfy the condition } T \\ \varnothing, \textit{ otherwise} \end{cases} \tag{2}$$

Therefore, $\tau_O(y)$ is the trivial opening associated with condition T. Trivial opening is used to extract the required connected components from image based on condition T. This operation removes the connected components which are not satisfied by the condition T. If connected component satisfied the condition T, then the entire region of that components are preserved. So shape and size are not disturbed by this opening. Trivial opening is mainly used for object detection and identification. Road areas can be easily filtered by trivial opening. Since high resolution image is considered for this work, roads appeared as identical region and long features in satellite images. So long feature roads can be extracted by selecting the condition as the long axes of minimum ellipse for trivial opening operation. The trivial opening for road detection is obtained using the following Equation 3.

$$\text{Ro} = \{P \mid \text{Long axis of axis of minimum ellipse enclosing } P(i) >= T\} \tag{3}$$

Where P is an image and $P(i)$ is a connected component of an image. Thus by using Equation 1, all the connected components of an image are extracted. From these connected components, road components are segmented using Equation 3. Thus, resultant image Ro has the connected road component which is greater than T.

2.3 Morphological closing

Matheron and Serra developed mathematical morphology approach which is based on set theory. Morphology is mainly used for extracting image components used for feature extraction such as boundaries, skeleton, and convex hull. Digital images can be processed using morphology based on geometrical shape [34]. Dilation and erosion are the most fundamental tools in morphological image processing [35,36]. Morphological dilation is an operation that grows or thickens objects in a binary image. The specific manner extent of this thickening is controlled by structuring element. Let Y be an image, and B is the structuring element, then the dilation of Y by B is denoted as in Equation 4.

$$Y \oplus B = \{z | (\hat{B})_z \cap Y = \varnothing\} \tag{4}$$

$\hat{B}$ is a reflection set of B, and it is given in the following 5.

$$\hat{B} = \{a | a = -b \; for \; b \in B\} \tag{5}$$

$(B)_z$ is a translation of set B, and it is given in Equation 6.

$$B_z = \{c | c = b + z \; for \; b \in B\} \tag{6}$$

$\varnothing$ is an empty set.

Morphological erosion shrinks or thins objects in a binary image. The extent of this shrinking is controlled by structuring element. The erosion of Y by B is denoted as in Equation 7.

$$Y \ominus B = \{z | (B)_z \subseteq Y\} \tag{7}$$

The erosion of Y by B is the set of all point z such that B translated by z is contained in Y. The various combinations of dilation and erosion such as morphological opening and closing are used in most of the image processing applications. Morphological closing of Y by B, defined as a dilation, is followed by erosion, and it is defined as in Equation 8. Geometrically, closing is the complement of the union of all translations of B that do not overlap Y.

$$Y \cdot B = (Y \oplus B) \ominus B \tag{8}$$

Connected component extraction produces connected road region, and this road region may have holes due to vehicles or tree shadows on the roads. Morphological closing is used to remove those holes on the road region. Thus, morphological closing is applied to the output of connected component extraction to fill the spaces inside the road region.

2.4 Morphological opening

The morphological opening of Y by B, defined as erosion, followed by dilation and same structuring element is used for both operations. Morphological opening of Y and B is defined as in Equation 9.

$$Y \circ B = (Y \ominus B) \oplus B \tag{9}$$

That can be written as $X \circ Y = \cup \{(Y)Z | (Y)z \subseteq X\}$. The opening of X by Y is the union of all translations of Y that fit entirely with X. Morphological opening is applied on resultant image from morphological closed operation to remove unwanted portions. The size of a structure element for opening operation must be smaller than main road width but slightly larger than unwanted path.

2.5 Morphological thinning

The thinning of a set A by a structuring element B, denoted A, can be defined in terms of the hit-or-miss transform as in Equation 10.

$$A \otimes B = A - (A \circledast B) = A \cap (A \circledast B)^C \tag{10}$$

Where $(A \circledast B)$ represent the hit-or miss transform of A and B. Morphological hit-or-miss transform is a fundamental tool for shape extraction. It is useful to identify specified configuration of pixels, such as isolated foreground pixels or pixels that are end points of line segments [37]. Hit-or-miss transform of Y and B is given in Equation 11.

$$Y * B = (Y \ominus B_1) \cap (Y^C \ominus B_2) \tag{11}$$

Where $B = (B_1, B_2)$, B_1 is the subset of B related with an object, and B_2 is the subset of B related with the corresponding background. Morphological thinning is applied on the output image of opening operation. It produced centerline of the road network but this extracted network consists of small unwanted edge segments. Further refinement is needed to remove this small edge segments. The unwanted small segments are removed using lookup table operations. Lookup table operation is also a morphological task. The length of road edge segments is calculated; and if length of edge segment is less than the given threshold value, then that edge segment is removed. Finally road centerline is extracted from the given high resolution satellite images.

2.6 Performance evaluation of road extraction

The performance of the proposed road extraction is observed by calculating the performance measures such as completeness, correctness, and quality. To measure these parameters, extracted road network is compared with manually drawn ground truth road map [38]. A constant width buffer is formed around the reference ground truth road map. The portion of the extracted road data which is lying inside the buffer area is known as matched extraction as shown in Figure 3a. The matched extracted road data are calculated as true positive (TP), and the unmatched extracted data is calculated as false positive (FP). Then the buffer is formed around the extracted road data, and the portion of the reference data within the buffer is known as matched reference as shown in Figure 3b. The length of matched portion is equal to true positive (TP). The unmatched reference data are calculated as false negative (FN).

2.6.1 Performance measures

Performance measures such as completeness, correctness, and quality are the most important parameters for the evaluation of the road extraction.

2.6.1.1 Completeness The completeness is the ratio between matched reference road data with total length of reference road map. The completeness is calculated by using the following Equation 12.

$$\text{Comp}\,\% = \frac{\text{length of matched reference}}{\text{length of reference}} \cong \frac{\text{TP}}{\text{TP}+\text{FN}} * 100 \tag{12}$$

2.6.1.2 Correctness The correctness represents the percentage of correctly extracted road data, i.e., the ratio between matched parts of extracted road network with total length of extracted road network. The correctness is measured by using the following Equation 13.

$$\text{Corr}\,\% = \frac{\text{length of matched extraction}}{\text{length of extraction}} \cong \frac{\text{TP}}{\text{TP}+\text{FP}} * 100 \tag{13}$$

2.6.1.3 Quality The goodness of the road extraction result is measured using the quality measures. It considered both completeness and correctness of the extracted data. The value of quality is calculated by using the following Equation 14.

$$\text{Qual}\,\% = \frac{\text{length of matched extraction}}{\text{length of extracted data} + \text{length of unmatched reference}} \cong \frac{\text{TP}}{\text{TP}+\text{FP}+\text{FN}} * 100 \tag{14}$$

3 Experimental results and discussion

The proposed methodology is applied on satellite images collected from Satellite Imaging Corporation and Apollo Mapping [39,40]. The results of different steps of the proposed method for test image 1 are given in Figure 4. The approximate road regions are segmented using adaptive global thresholding technique. Threshold values are found using the histogram of test image 1. Test image is shown in Figure 4a, and the segmented result using adaptive global thresholding technique is given in Figure 4b. The resultant road region segmented image consists of some unwanted regions. Morphological operators are used for further processing to remove this unwanted road regions. Connected component of this segmented image is obtained using Equation 8. This connected component consists of road and non-road components. Most of the non-road components are removed, and road components are extracted using trivial opening method by applying Equation 10 and resultant image shown in Figure 4c.

The resultant image has holes due to objects on roads or tree shadows which is shown in green circled portion on Figure 4c. These holes can be closed using morphological closing operations, and the result is given in Figure 4d; closed portions are highlighted by green circle. The resultant image is further filtered using morphological opening operation to remove unwanted portions. The size of the structure element for opening operation must be smaller than main road but slightly larger than unwanted path. The morphological opened result is shown in Figure 4e. After that, thinning operation is

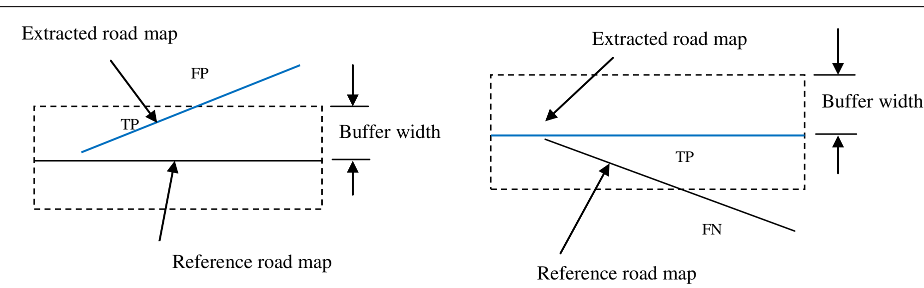

(a) Matched extraction (b) Matched reference

Figure 3 Matched extraction (a) and matched reference (b).

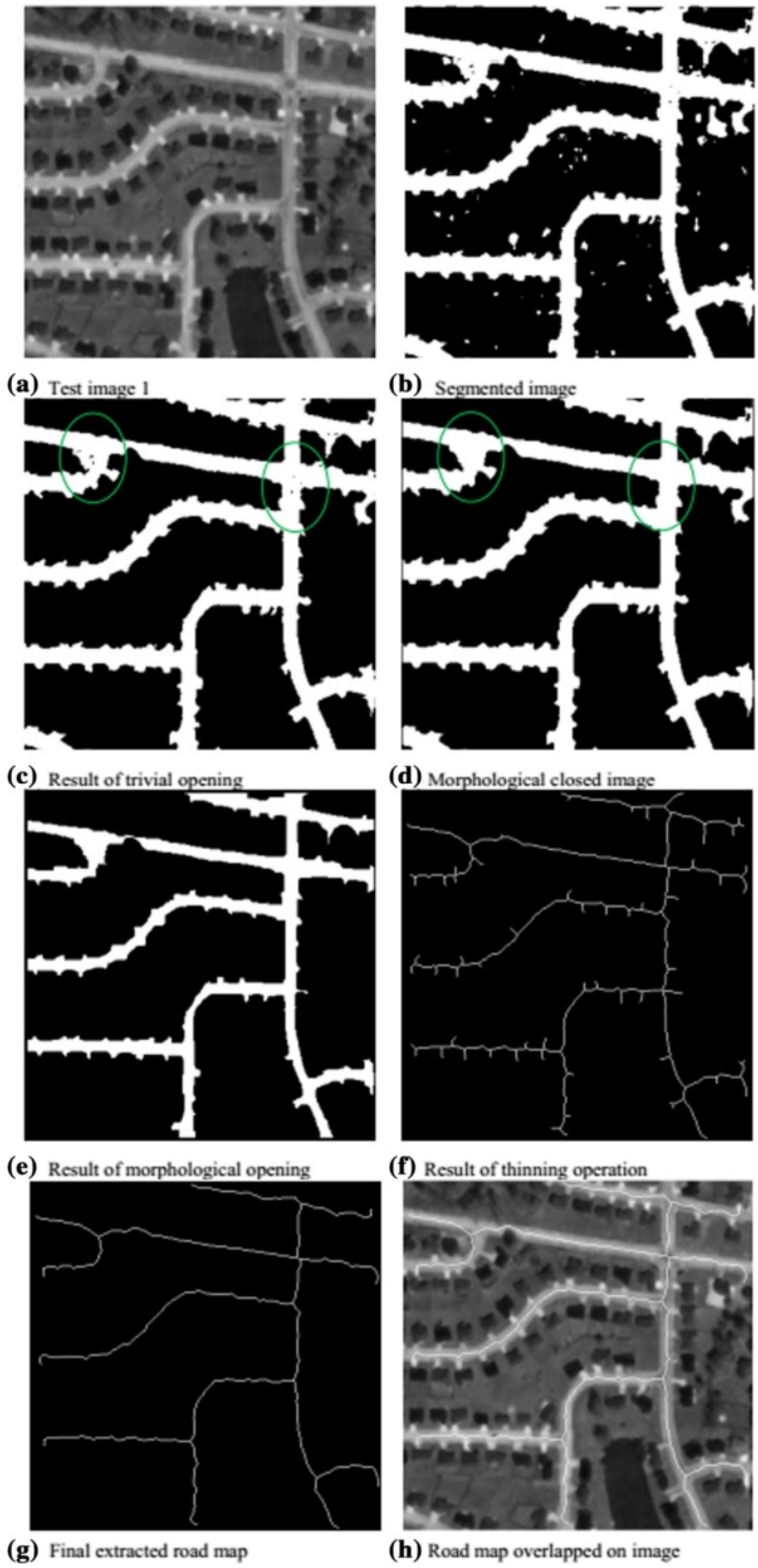

Figure 4 Experimental results of proposed methodology. (a) Test image 1, **(b)** segmented image, **(c)** result of trivial opening, **(d)** morphological closed image, **(e)** result of morphological opening, **(f)** result of thinning operation, **(g)** final extracted road map, **(h)** road map overlapped on image.

applied to extract centerline of the road network which is shown in Figure 4f. Since this thinned road network consists of unwanted small edge segments, further refinement on resultant image is needed. The length of road edge segments is calculated; and if length of edge segment is less than given threshold value, then that edge segment is removed. The resultant final road map is shown in Figure 4g. The extracted road map is overlapped on original satellite input image, and it is given in Figure 4h.

The proposed algorithm is implemented on noisy satellite image, and the result is given in Figure 5. For easy comparison, the same test image 1 is taken for this implementation which is used in Figure 4. Test image 1 is given in Figure 5a, and that image is contaminated by salt and pepper noise at 5% noise density level, the

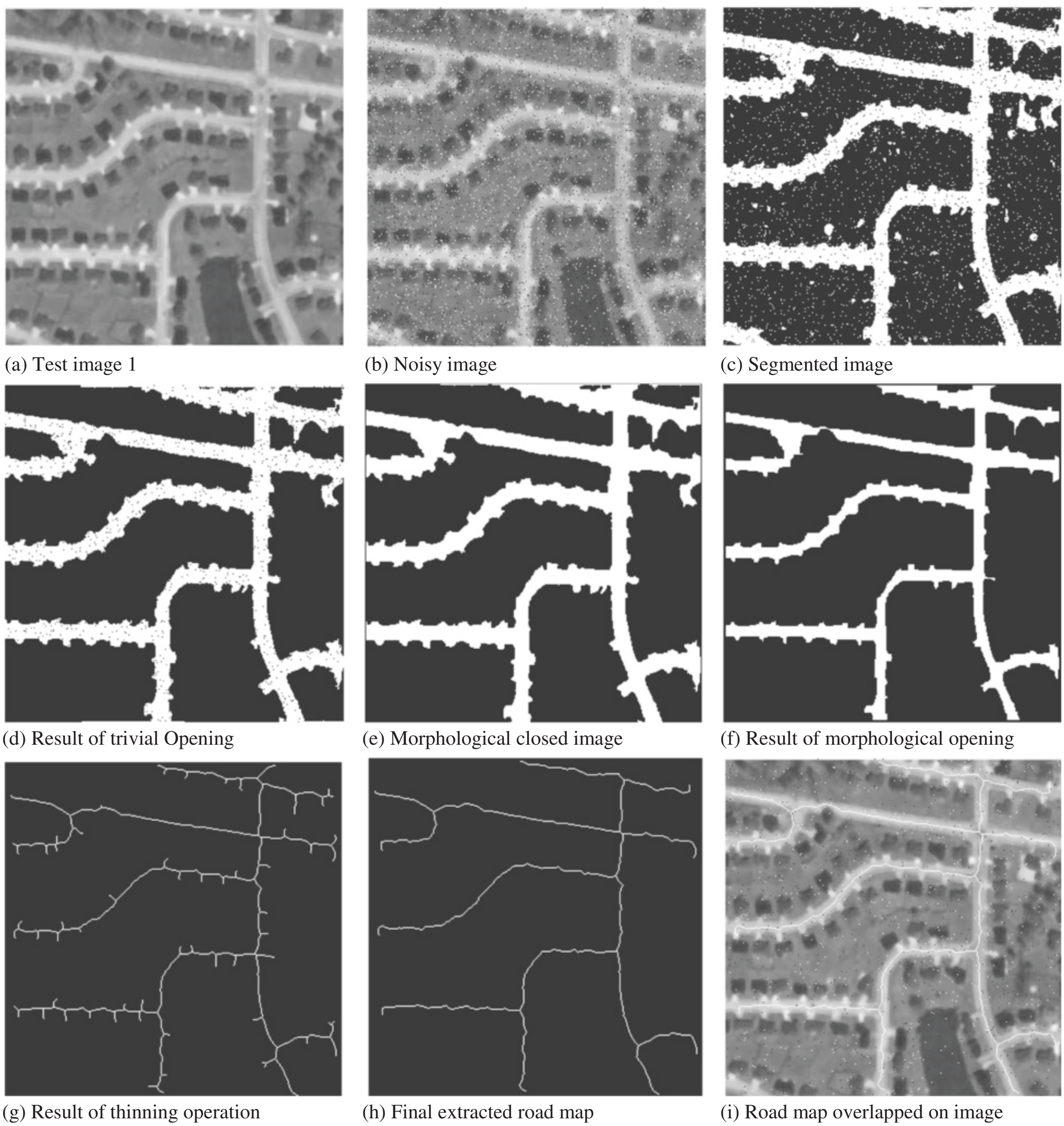

Figure 5 Experimental results of proposed methodology in noisy images. **(a)** Test image 1, **(b)** noisy image, **(c)** segmented image, **(d)** result of trivial opening, **(e)** morphological closed image, **(f)** result of morphological opening, **(g)** result of thinning operation, **(h)** final extracted road map, **(i)** road map overlapped on image.

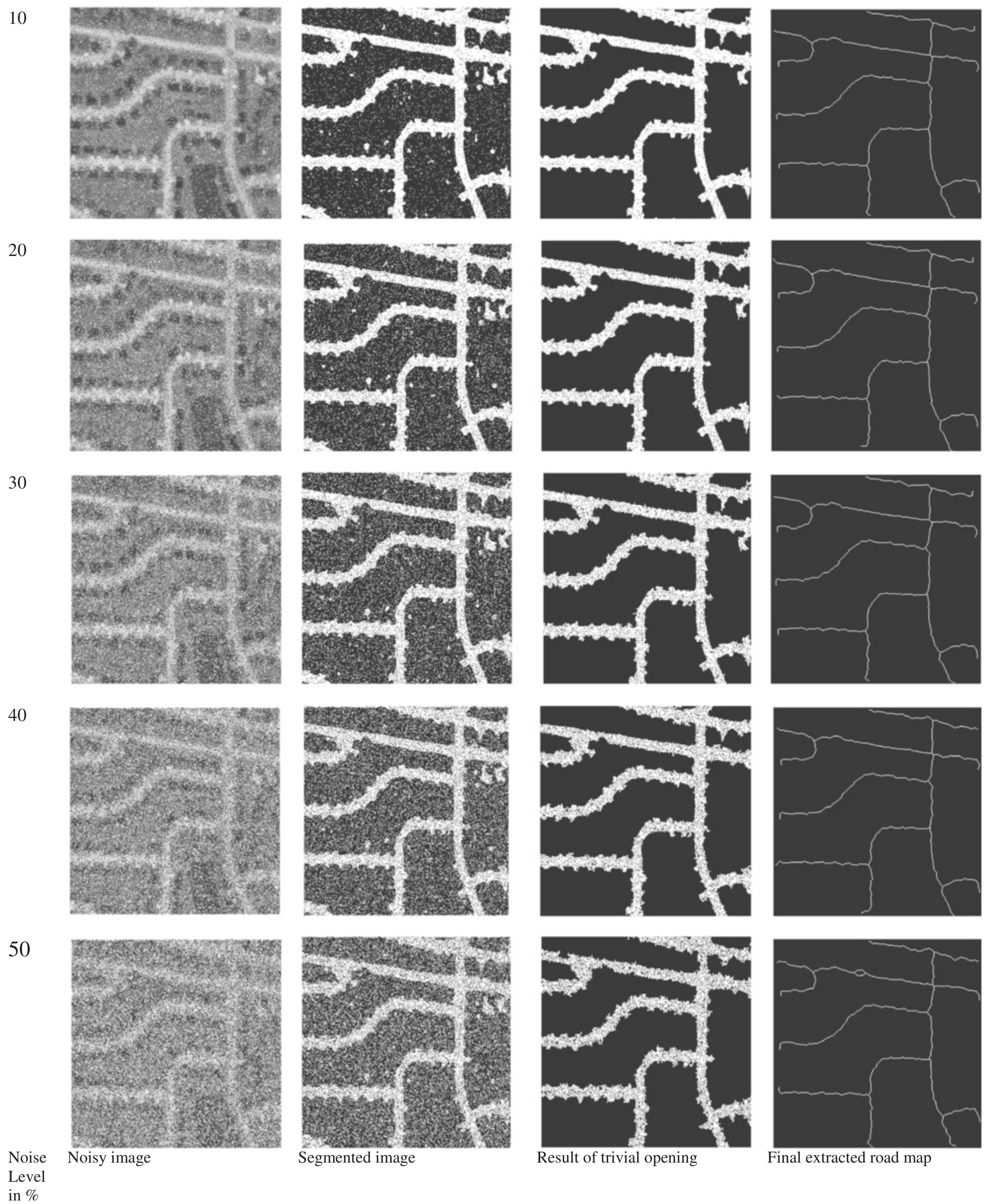

Figure 6 Experimental results of proposed methodology in noisy images at various noise density levels.

resultant noisy image is shown in Figure 5b. The road regions are segmented from this noisy image using adaptive global thresholding method, the pepper noise pixels in non-road regions are removed because of thresholding operation, and some noise pixels are presented along with road region in segmented image as shown in Figure 5c. The trivial opening is applied to remove non-road regions as discussed in earlier, and during this process along with non-road regions, noises are also removed.

Resultant trivial opening operation is given in Figure 5d. Now, noises are presented only on the road regions that can be eliminated by using morphological closing operation as shown in Figure 5e. At present, all the salt and pepper noise pixels are removed from image. Further processing is applied to detect road network such as morphological opening and thinning; result is given in Figure 5f and g, respectively. Small edge segments are removed as shown in Figure 5h, and final detected road network is overlapped on noisy image as given in Figure 5i. Thus, the proposed work is the noise-immune algorithm for road centerline extraction.

The proposed work is implemented on noisy images at various noise density levels from 10% to 50%, and results

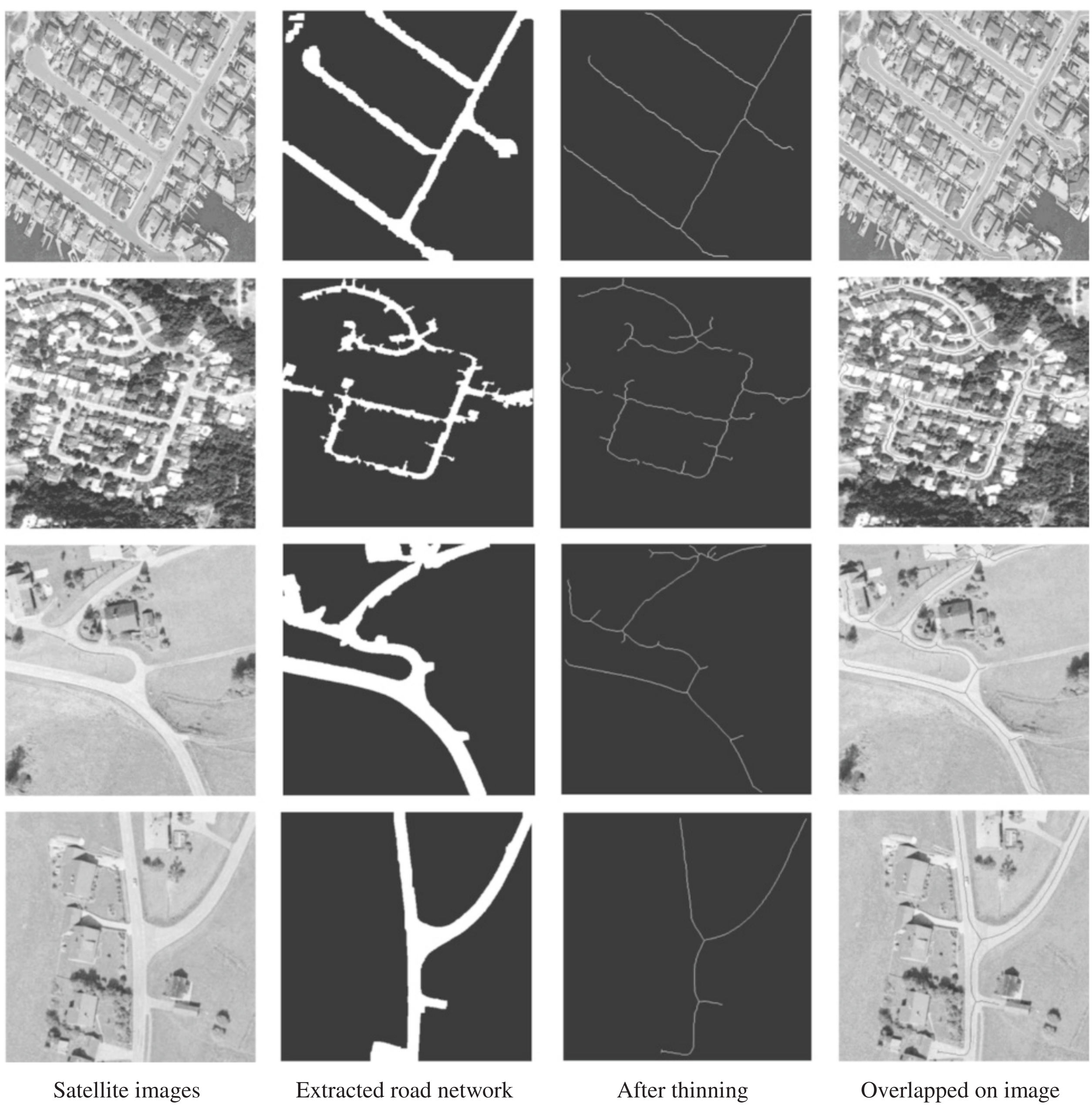

Figure 7 Results of proposed algorithm for various satellite images.

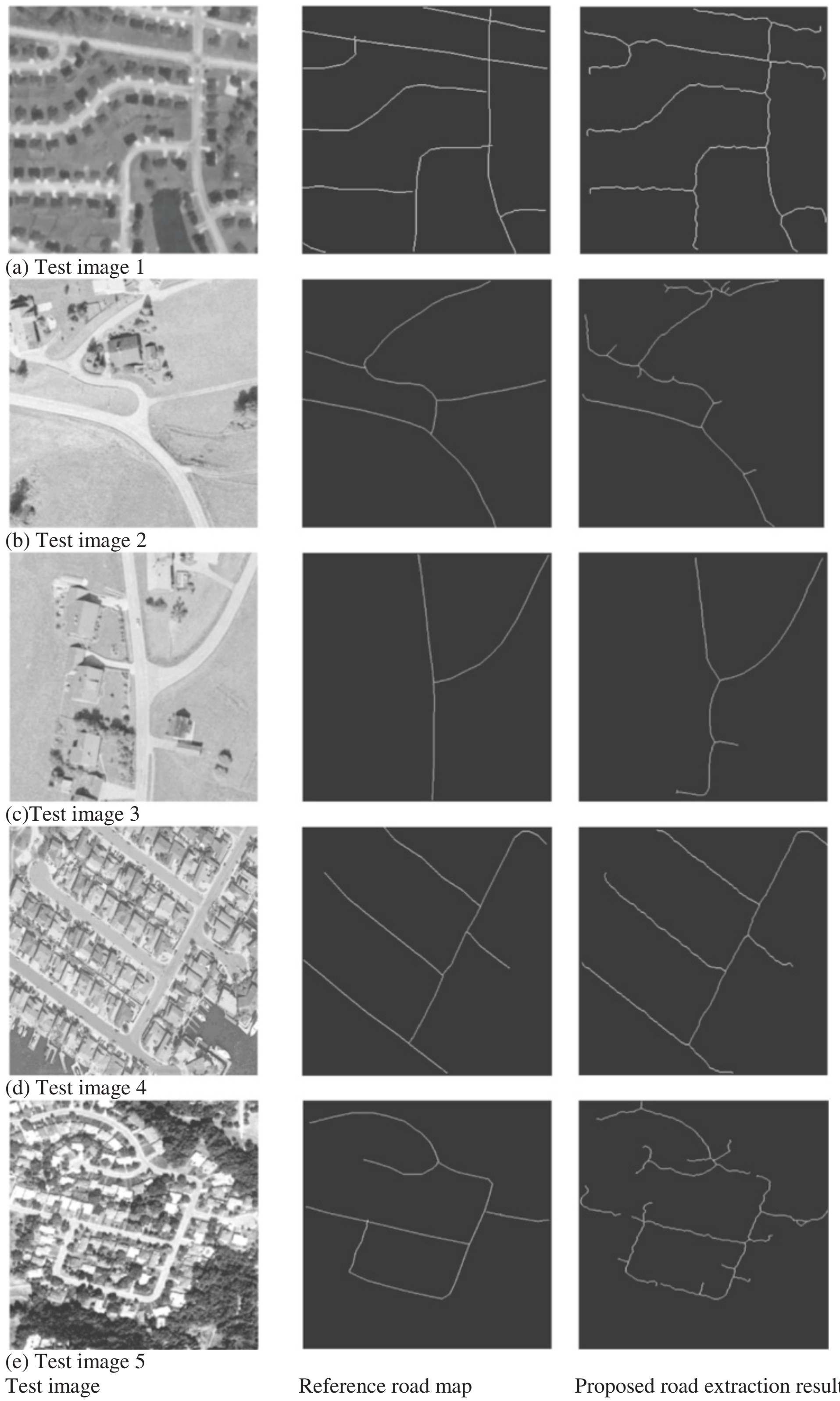

Figure 8 Performance evaluation of result with ground truth reference road map. For **(a)** test image 1, **(b)** test image 2, **(c)** test image 3, **(d)** test image 4, and **(e)** test image 5.

are given in Figure 6. Noisy images at various noise density levels at 10%, 20%, 30%, 40%, and 50%, corresponding intermediate results such as road segmentation, and result after trivial opening and final extracted road map are shown in Figure 6. The final extracted road map in all noisy level is almost equal to noiseless result. Thus, this result shows that the proposed work produces road map output equal to noiseless image at the noise levels up to 50% and it proves that this work is insensitive to salt and pepper noise.

The proposed method is implemented on various other high resolution images, and the corresponding results are given in Figure 7. Satellite images, corresponding extracted road network by using proposed method, corresponding extracted road centerline using thinning, and removal of small segment and overlapping of extracted results with original satellite image are shown in Figure 7. This shows that proposed road centerline extraction provides the best result for almost all the images.

3.1 Calculation of performance measures

The performance of proposed extracted road network is compared with ground truth road map which is a manually drawn road map. Digitized manually drawn road map can be obtained using the software GIMP (GNU Image Manipulation Program). GIMP is a high quality freely available software for image processing applications [41]. Ground truth road map is plotted by using GIMP software. The proposed results are compared with these reference road maps, and this comparison is given in Figure 8.

The performance measures such as completeness, correctness, and quality are evaluated for proposed work on various test images. For this comparison, true positive, false positive, and true negatives are calculated for each test images. As shown in Figure 3, manually drawn reference road map is compared with extracted road network and buffer width is set as 3. Then, the value of TP, FP, and FN is counted based on the following consideration.

- TP - true positive, an element present in ground truth and extracted road network
- FP - false positive, an element present in extracted road network but not in ground truth
- FN - false negative, an element present in ground truth but not in extracted road network

By using these values, completeness, correctness, and quality measures are calculated using the Equations 12, 13, and 14. These performance measures are evaluated for proposed work on various test images. In order to compare with others work, the measures are calculated in terms of percentage and round off to the nearest integer. The results are tabulated in Table 1. The performance measures show that the lowest value of completeness is 87% and the maximum value is 95%, and correctness measures show that all the values are above 94%. Similarly, quality measures lie between 83% and 93%.

Table 1 Performance measures of proposed methodology with reference road map

Images	Completeness %	Correctness %	Quality %
Test image 1	89	99	89
Test image 2	87	94	83
Test image 3	89	95	85
Test image 4	95	98	93
Test image 5	90	95	86
Average	*90*	*96*	*87*

The performance measures are also evaluated for proposed work on noisy images of test image 1 at various noise density levels, and those values are tabulated in Table 2. The measures are compared with noiseless image, and minimal differences are there. This comparison shows that the maximum difference in completeness, correctness, and quality values is around 1% with noiseless values. Thus, the proposed work is appropriate for road centerline detection in noisy images also.

In proposed work, five test images are taken to measure the performance measures, and the number of images taken for these measures varies in other works. Thus for comparison with other works, minimum, maximum and average values for completeness, correctness and quality are considered. For easy to comparison, performance measures of all other methods are considered in terms of percentage.

Jiuxiang et al. [1] proposed road network detection, and their work is evaluated on five images and performance measures are tabulated; from that work, minimum and maximum values of completeness, correctness, and quality are taken and average values are calculated. Mena et al. [20] proposed an automatic road extraction approach. Performance measures are tabulated for five images in their work. From that table, minimum, maximum, and average values are noted. Another road

Table 2 Performance measures of proposed methodology for noisy images at various noise levels

Noise levels in %	Completeness %	Correctness %	Quality %
0	89.3	99.2	88.6
5	89.3	99.2	88.6
10	89.3	99.2	88.6
20	89	99.1	88.2
30	88.7	99.1	88
40	88.5	99.1	87.7
50	88.2	98.9	87.4

Table 3 Comparison of performance measures of proposed methodology with other methods

Methods	Completeness %			Correctness %			Quality %		
	Min	Max	Average	Min	Max	Average	Min	Max	Average
Jiuxiang [1]	84	94	91	81	96	90	82	92	85
Mena [20]	66	91	81	65	96	87	48	87	73
Rohit [25]	58	93	73	35	85	69	28	75	56
Zelang [21]	73	97	87	75	100	92	59	96	83
Wenzhong [22]	71	87	79	68	84	77	59	72	63
Xiaoying [3]	70	86	78	70	92	80	58	80	66
Zhijian [4]	80	92	87	82	89	89	68	83	76
Proposed work	*87*	*95*	*90*	*94*	*99*	*96*	*83*	*93*	*87*

extraction using K-means clustering and morphological operation is presented by Rohit et al. [25].

Completeness, correctness, and quality measures are calculated for ten different images, and the values are tabulated in their work. Minimum and maximum values in terms of percentage are taken from their work, and average values are calculated. Zelang et al. presented road extraction method based on tensor voting, kernel density estimation, and subspace constrained mean shift [21]. Completeness, correctness, and quality measures that are evaluated for four images are given in their paper. Wenzhong et al. proposed a method for road extraction by using spectral-spatial classification and shape features [22]. The minimum, maximum, and average values of performance measures are taken from their work. Xiaoying et al. presented an information fusion-based approach for road extraction [3], and quality measures are evaluated in that work. A feature fusion-based method for road extraction is proposed by Zhijian et al. [4]. Performance measures are calculated for various images from those values. Minimum, maximum, and average values are taken for comparison and given in Table 3. All the above results of existing works along with proposed work results are tabulated as shown in Table 3 for comparison. In Table 3, all the values are rounded to nearest integer.

Sahar et al. evaluated completeness and correctness for their work, and quality measures are not calculated [18]. From their measures, the maximum value of completeness is 92% and correctness is 98%, which is lesser than the proposed work maximum values shown in Table 3. Boshir et al. [27] evaluated correctness measures in their work; completeness and quality measures are not given. From those measures, minimum value of correctness is 92.82% and average value is 95.71% which is lesser than the proposed work. Maximum value is 100% but proposed work has 99%. Pankaj et al. calculated correctness and completeness values for only one image [24]. The correctness and completeness values are 96.52% and 95.32%, respectively. From Table 1, for test image 4, the correctness and completeness values are 98% and 95%, respectively. In some work, performance measures are not evaluated [17,19,23,31,32,34]. So those works are not taken for comparison with the proposed work.

This comparison table is plotted to enhance the difference clearly, and the plot is shown in Figure 9. The X-axis is divided into three portions: first portion shows the minimum, maximum, and average values of completeness;

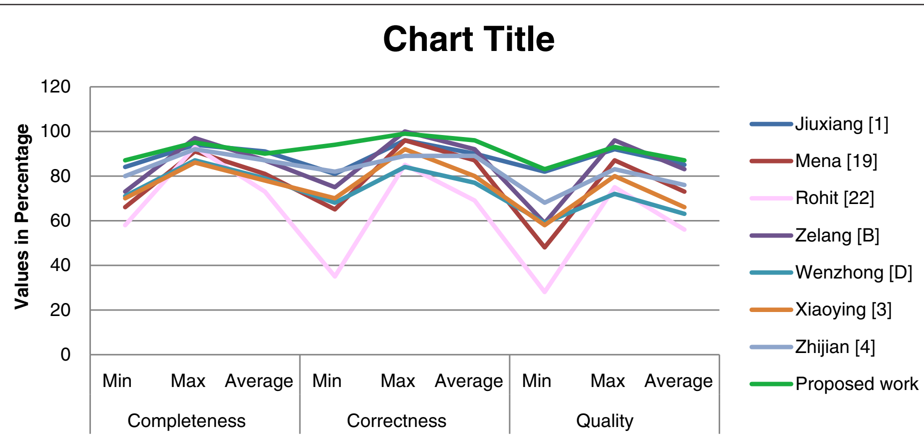

Figure 9 Comparison plot for performance measures.

second portion shows the minimum, maximum, and average values of correctness; and third portion shows the minimum, maximum, and average values of quality values. The Y-axis has shown the corresponding values in percentage. The graph is plotted for the comparison of completeness, correctness, and quality of various algorithms with the proposed work. In this plot, the proposed work lies on top level than other methods. Thus, this comparison in Table 3 and Figure 9 proved that the proposed method gives higher result than other methods.

4 Conclusions

Road centerline extraction of high resolution satellite images using connected component-based trivial opening operation along with morphological operation is proposed in this work. The proposed work includes the following steps such as segmentation of approximated road regions from satellite image using adaptive global threshold method, the use of connected component analysis to extract connected objects from that image, and application of trivial opening with the criteria of long axis of minimum ellipse of connected component to extract connected road component from connected objects of that image. For further refinement, morphological opening is applied using structure element which is equal to the width of a road. Final extracted network consists of entire road region. Thinning is applied to detect the centerline of road network. The proposed method is implemented on various satellite images, and results are given. These results prove that the proposed method is yielding very good results for all types of images. This method is also implemented on noisy images at various levels of noise density, and good results are obtained. This proves that the proposed method is insensitive to noise. The obtained results for various images are compared with manually plotted reference road map. Performance measures such as completeness, correctness, and quality are evaluated for different images, and values are tabulated in this work. The completeness values lie between 87% and 95%, correctness values lie between 94% and 99%, and quality measures lie between 83% and 93%. These comparisons prove that the proposed method provides the road network which is closer to reference road map. Performance measures are evaluated for noisy images at various levels, and those values are compared with noiseless image measures. This comparison shows that the proposed work produces good results for noisy images also. The performance measures are compared with other methods, and values are tabulated. Comparison plot is also shown which shows that proposed method values are higher than all other methods. Thus, this comparison proved that the proposed work provided very good results than other methods.

Abbreviations

CC: connected component; GIS: geographic information systems; TP: true positive; FP: false positive; TN: true negative; FN: false negative; GIMP: GNU Image manipulation program.

Competing interests

The authors declare that they have no competing interests.

Author details

[1]Department of Electronics and Communication Engineering, Sethu Institute of Technology, Madurai-Thoothukudi Highway, Kariapatti, Virudhunagar District 626115, Tamil Nadu, India. [2]Department of Electronics and Communication Engineering, Mepco Schlenk Engineering College, Mepco Nagar, Sivakasi 626005, Tamil Nadu, India.

Received: 25 September 2014 Accepted: 4 March 2015
Published online: 20 March 2015

References

1. J Hu, A Razdan, JC Femiani, M Cui, P Wonka, Road network extraction and intersection detection from aerial images by tracking road footprints. IEEE Trans. Geosci. Remote Sens. **45**(12), 4144–4157 (2007)
2. C Unsalan, B Sirmacek, Road network detection using probabilistic and graph theoretical methods. IEEE Trans. Geosci. Remote Sens. **50**(11), 4441–4453 (2012)
3. X Jin, CH Davis, An integrated system for automatic road mapping from high-resolution multi-spectral satellite imagery by information fusion. Inf. Fusion **6**(4), 257–273 (2005)
4. Z Huang, J Zhang, L Wang, F Xu, A feature fusion method for road line extraction from remote sensing image, in *Proceedings of the IEEE International Geoscience and Remote Sensing Symposium(IGARSS)* (IEEE, Munich, German, 2012), pp. 52–55
5. X Lin, Z Liu, J Zhang, J Shen, Combining multiple algorithms for road network tracking from multiple source remotely sensed imagery: a practical system and performance evaluation. Sensors **9**, 1237–1258 (2009)
6. AP Dal Poz, RB Zanin, GM d Vale, Automated extraction of road network from medium-and high-resolution images. Pattern Recog. Image Anal. **16**(2), 239–248 (2006)
7. A Baumgartner, S Hinz, C Wiedemann, Efficient methods and interfaces for road tracking. Inter. Arch. Photogramm. Remote Sens. Spatial. Inf. Sci. **34**(3/B), 28–31 (2002)
8. A Gruen, H Li, Semi-automatic linear feature extraction by dynamic programming and LSB-snakes. Photogramm. Eng. Remote Sens. **63**(8), 985–994 (1997)
9. AP Dal Poz, GM Do Vale, Dynamic programming approach for semi-automated road extraction from medium-and high-resolution images, in *Proceedings of the ISPrS Archives, Vol. 34, part 3* (ISPRS, Munich, German, 2003), pp. 87–91. 17–19
10. H Zhao, J Kumagai, M Nakagawa, R Shibasaki, Semi-automatic road extraction from high-resolution satellite image. Remote Sens. Spatial Inf. Sci. **34**(3/A), 406–411 (2002)
11. Z Miao, B Wang, W Shi, H Zhang, A semi-automatic method for road centerline extraction from VHR images. IEEE Trans. Geosci. Remote Sens. Lett. **11**(11), 1–5 (2014)
12. Z Miao, W Shi, H Zhang, X Wang, Road centerline extraction from high-resolution imagery based on shape features and multivariate adaptive regression splines. IEEE Geosci. Remote Sens. Lett. **10**(3), 583–587 (2013)
13. J Senthilnath, M Rajeshwari, SN Omkar, Automatic road extraction using high resolution satellite image based on texture progressive analysis and normalized cut method. J. Indian Soc. Remote Sens. **37**, 351–361 (2009)
14. X Huang, L Zhang, Road centerline extraction from high-resolution imagery based on multiscale structural features and support vector machines. Int. J. Remote Sens. **30**(8), 1977–1998 (2009)
15. H Jin, M Miska, E Chung, M Li,Y Feng, in *Remote Sensing - Advanced Techniques and Platforms* ed. by B Escalante-Ramirez. Road feature extraction from high resolution aerial images upon rural regions based on multi-resolution image analysis and Gabor filters. (ISBN: 978-953-51-0652-4, InTech, 2012), p. 387–416
16. S Das, TT Mirnalinee, K Varghese, Use of salient features for the design of a multistage framework to extract roads from high-resolution multispectral satellite images. IEEE Trans. Geosci. Remote Sens. **49**(10), 3906–3931 (2011)
17. T Chen, W Ji, K Zhang, A wavelet transform based method for road centerline extraction. Photogramm. Eng. Remote Sens. **70**(12), 1423–1431 (2004)

18. S Movaghati, A Moghaddamjoo, A Tavakoli, Road extraction from satellite images using particle filtering and extended Kalman filtering. IEEE Trans. Geosci. Remote Sens. **48**(7), 2807–2817 (2010)
19. T Geraud, JB Mouret, Fast road network extraction in satellite images using mathematical morphology and Markov random fields. EURASIP J. Appl. Signal Proc. **16**, 2503–2514 (2004)
20. JB Mena, JA Malpica, An automatic method for road extraction in rural and semi-urban areas starting from high resolution satellite imagery. Pattern Recog. Lett. **26**, 1201–1220 (2005)
21. Z Miao, B Wang, W Shi, H Wu, *A method for accurate road centerline extraction from a classified image* (IEEE J. Selected Topics Appl, Earth Observations Remote Sens, 2014). doi: 10.1109/JSTARS.2014.2309613
22. W Shi, Z Miao, Q Wang, H Zhang, Spectral-spatial classification and shape features for urban road centerline extraction. IEEE Trans. Geosci. Remote Sens. Lett. **11**(4), 788–792 (2014)
23. S Valero, J Chanussot, JA Benediktsson, H Talbot, B Waske, Advanced directional mathematical morphology for the detection of the road network in very high resolution remote sensing images. Pattern Recog. Lett. **31**, 1120–1127 (2010)
24. PP Singh, RD Garg, Automatic road extraction from high resolution satellite image using adaptive global thresholding and morphological operations. J. Indian Soc. Remote Sens. **41**(3), 631–640 (2013)
25. R Maurya, PR Gupta, AS Shukla, Road extraction using K-means clustering and morphological operations, in *Proceedings of the IEEE International Conference on Image Information Processing* (IEEE, Himachal Pradesh, India, 2011)
26. C Zhu, W Shi, M Pesaresi, L Liu, X Chen, B King, The recognition of road network from high resolution satellite remotely sensed data using image morphological characteristics. Int. J. Remote Sens. **26**, 5493–5508 (2005)
27. B Ahmed, MF Rahman, Automatic road extractions from high resolution satellite imagery using road intersection model in urban areas. Comput. Eng. Intell. Syst. **2**(4), 82–93 (2011)
28. MD Mura, JA Benediktsson, B Waske, L Bruzzone, Morphological attribute profiles for the analysis of very high resolution images. IEEE Trans. Geosci. Remote Sens. **48**(10), 3747–3762 (2010)
29. M Boldt, K Schulza, A Thiele, S Hinz, Using morphological differential attribute profiles for change categorization in high resolution SAR images. Inter. Arch. Photogramm. Remote Sens. Spatial Inf. Sci. **1**(1), 29–34 (2013)
30. B Sowmya, B Sheelarani, Hybrid technique for automatic main road extraction. National J. Electromic Sci. Syst. **1**(2), 55–60 (2010)
31. A Mohammadzadeh, A Tavakoli, MJ Valadan, Zoej, Road extraction based on fuzzy logic and mathematical morphology from pan-sharpened IKONOS images. The photogram Record **21**(113), 44–60 (2006)
32. A Mohammadzadeh, A Tavakoli, MJ Valadan Zoej, Automatic linear feature extraction of Iranian roads from high resolution multi-spectral satellite imagery, in *Proceedings of the XXth ISPRS Congress* (ISPRS, Istanbul, Turkey, 2004), pp. 764–768
33. J Serra, L Vincent, An overview of morphological filtering. Circuits, Syst. Signal Proc. **11**(1), 47–108 (1992)
34. C Zhang, S Murai, EP Baltsavias, in Proceedings of the *ISPRS Workshop on 3D Geospatial Data Production: Meeting Application Requirements*. Road network detection by mathematical morphology, (France, 1999), p. 185–200
35. RC Gonzalez, RE Woods, *Digital image processing*, 2nd edn. (India, Prentice Hall, 2002)
36. JA Benediktsson, M Pesaresi, K Arnason, Classification and feature extraction for remote Sensing images from urban areas based on morphological transformations. IEEE Trans. Geosci. Remote Sens. **41**(9), 1940–1949 (2003)
37. GVR Reddy, V VijayaKumar, MA Reddy, Morphological texture synthesis algorithm using pixel and patch based approach. Int. J. Sci. Eng. Res. **3**(2), 1–4 (2012)
38. C Heipke, H Mayer, C Wiedemann, O Jamet, Evaluation of automatic road extraction. Inter. Arch. Photogramm. Remote Sens. **32**(3), 151–160 (1997)
39. Satellite images from Satellite Imaging Corporation (SIC). Available: http://www.satimagingcorp.com
40. Satellite images from Apollo Mapping. Available: https://www.apollomapping.com
41. RW Solomon, Free and open source software for the manipulation of digital images. Am. J. Roentgenol. **192**(6), 330–334 (2009)